

# The Space Infrared Interferometric Telescope (SPIRIT): Optical System Design Considerations

Mark E. Wilson\*<sup>a</sup>, David Leisawitz, Anthony J. Martino, Stephen Rinehart, Julie Crooke,  
June Tveekrem, Jason Budinoff, Tupper Hyde

<sup>a</sup>NASA Goddard Space Flight Center, Greenbelt Rd. , Greenbelt, MD. 20771

## ABSTRACT

The Space Infrared Interferometric Telescope (SPIRIT) was designed to accomplish three scientific objectives: (1) learn how planetary systems form from protostellar disks and how they acquire their inhomogeneous chemical composition; (2) characterize the family of extrasolar planetary systems by imaging the structure in debris disks to understand how and where planets of different types form; and (3) learn how high-redshift galaxies formed and merged to form the present-day population of galaxies. SPIRIT will accomplish these objectives through infrared observations with a two aperture interferometric instrument. This paper gives an overview into the optical system design, including the design form, the metrology systems used for control, stray light, and optical testing.

Keywords: SPIRIT, Infrared/IR, Interferometry, Telescope, Optical Design

## INTRODUCTION

The Space Infrared Interferometric Telescope (SPIRIT) was designed to accomplish three scientific objectives: (1) learn how planetary systems form from protostellar disks and how they acquire their inhomogeneous chemical composition; (2) characterize the family of extrasolar planetary systems by imaging the structure in debris disks to understand how and where planets of different types form; and (3) learn how high-redshift galaxies formed and merged to form the present-day population of galaxies. To achieve these objectives SPIRIT will provide integral field spectroscopy throughout the wavelength range 25 – 400  $\mu\text{m}$  with sub-arcsecond angular resolution and  $\lambda/\Delta\lambda = 3000$  spectral resolution in a 1 arcminute instantaneous field of view. Many of the astronomical targets of interest will be resolved for the first time at far-IR wavelengths. SPIRIT's spatially resolved spectra will break model degeneracy and enable a new physical understanding of forming stars and planetary systems, mature planetary systems, and galaxies.

A single scientific instrument gives SPIRIT its powerful combination of spatial and spectroscopic measurement capabilities. SPIRIT is a Michelson stellar interferometer with a scanning optical delay line for Fourier transform spectroscopy and compensation of external optical path length differences. Following beam combination in the pupil plane, detector arrays multiplex the area coverage, expanding the field of view from the diffraction spot size of the individual light collecting telescopes to the desired arcminute scale. SPIRIT's two telescopes can be moved to sample many interferometric baselines, and therefore spatial structure on all of the angular scales necessary to produce high-quality far-IR images. The image resolution, 0.3 ( $\lambda/100 \mu\text{m}$ ) arcsec, is determined by the maximum baseline length, 36 m. To attain superlative sensitivity, limited by astrophysical background photon noise, the SPIRIT optics are cooled to 4 K and sufficiently sensitive detectors will be used.

The results of a pre-Formulation Phase study of the SPIRIT mission concept are given in a series of papers, of which this paper is one. The scientific objectives, measurement requirements, and an overview of the design concept are described by Leisawitz et al. (2007). [1] Hyde et al. (2007) [2] summarize system level trades and describe the design concept in greater detail, including the error budget for key design parameters and model-based estimates of the system performance. Budinoff et al. (2007) [3] describes the SPIRIT mechanical design and mechanisms and explains how the mechanical design will meet instrument stability, thermal and packaging requirements. DiPirro et al. (2007) [4] present the thermal design concept, thermal modeling results, and the cooling power requirements, and they explain how cryocoolers will be used to meet these requirements. Benford et al. (2007) [5] describe detector requirements, including NEP, pixel count and readout speed, and present the rationale for using small arrays of TES bolometers. Rinehart et al. (2007) [6] update the status of our development of the wide-field imaging interferometry technique applicable to SPIRIT, and Martino et al. (2007) [7] describe a model of the Wide-field Imaging Interferometry Testbed, a model

which can be adapted to simulate interferometric data from SPIRIT. This paper focuses on the trades that influence optical system design choices, stray light control, metrology, and optical system performance verification.

## 2.0 OPTICAL DESIGN

The SPIRIT optical system consists of a pair of afocal collecting telescopes whose beams are combined in the pupil plane located inside a beam combiner volume. Because of the large size of the beams at the aperture of collecting telescopes, it is necessary to demagnify the size down to a value consistent with manufacturing constraints on metal mesh dichroic beamsplitters and glass beamsplitters used as 50/50 amplitude beamsplitters. For SPIRIT, this meant a two stage demagnification: one at the collector telescope itself and another located in the central beam combining volume.

### 2.1 Collecting telescopes

Each of the collecting telescopes, as shown in Figures 1 & 2, consists of a pair of afocal parabolas, used in a Cassegrain configuration, plus a fold flat used for coarse beam steering. They were chosen to be afocal to accommodate the variation in length between them as they move on the trolleys [3]. The determination of primary mirror diameter involved studies of several factors: what would fit in the launch vehicle (the Atlas V and Delta IV H vehicles were examined), collecting area vs. measurement integration time, mirror diameter vs. boom length (a tradeoff of sensitivity vs. angular resolution, with emphasis being on angular resolution), and fabrication/testing ease. A 1 meter diameter aperture was selected after balancing all the factors mentioned above. In order to avoid wavelength dependent diffraction effects from a central obscuration plus mounting structures for the secondary mirror, an off axis design was chosen. The field of view was also an important consideration; there were several values used (in the several arc minute range), with an overall field of view of 1 arc minute (full field) selected. From the optical perspective, this was selected primarily because of 2 limitations: size of metal mesh beamsplitters that can be manufactured, and the opening in the beam combiner structure (with resultant thermal issues). Table 1 shows the final design requirements.

Optical System Requirement	Value
Aperture	1000 mm (each collector primary mirror)
Field of View	1x1 arcmin (full field)
Wavelength Band	25-400 microns
Max telescope separation (center to center)	36 m
Min telescope separation (center to center)	6 m

**Table 1 – Optical Design Requirements**

An important factor in the design of the collector telescope is the beam size at the interferometer optics, particularly the divergence as it exits the collector telescope. The divergence calculation was based primarily on geometric optics considerations, as shown in the following equation; the goal is to minimize the beam diameter at the beam combiner entrance while ensuring that the spacecraft fits in the fairing and the simplifying the fabrication of the primary mirror

$$D_{\text{comb}} = (D_{\text{coll}}/m) + 2*B*\sin(m*FOV/2), \text{ where} \tag{1}$$

$D_{\text{comb}}$  = Diameter of beam at combiner primary

$D_{\text{coll}}$  = Diameter of beam at collector primary

$m$  = (de)magnification (>1 ;e.g. a value of 10 demagnifies the beam leaving the collector by a factor of 10

$B$  = Boom Length (same units as beam diameters, typically meters)

$FOV$  = full field of view (radians)

For  $D_{\text{coll}} = 1000$  mm,  $B = 36000$  mm, and  $\text{FOV} = 1$  arcmin, Figure 3 shows the variation of the beam diameter at the entrance to the beam combiner as a function of collector telescope magnification. This shows the beam diameter is minimized for  $m = 10$ ; this value also allowed the telescope assembly to fit into the fairing. A simple diffraction analysis of the beam indicated beam spreading of a few mm; this was neglected in determining the magnification to use. The flat mirror of the collector is used as a steering mirror to ensure that the beam travels parallel to the boom. For this design, it was found that the minimum unvignetted field of view is 3 arcminutes.

The primary mirror is an fast off axis parabola, with an  $f$ -number faster than  $f/1$ . It was felt that the mirror fabrication would be within standard practices. The rms wavefront error tolerance of the mirror is 50 nm. This tolerance was driven by the metrology systems (see Section 2.5), rather than the actual science measurements<sup>2</sup>. No focus or tip/tilt mechanism on the secondary was deemed necessary, that the proper alignment could be achieved through shims and other standard optical alignment techniques.

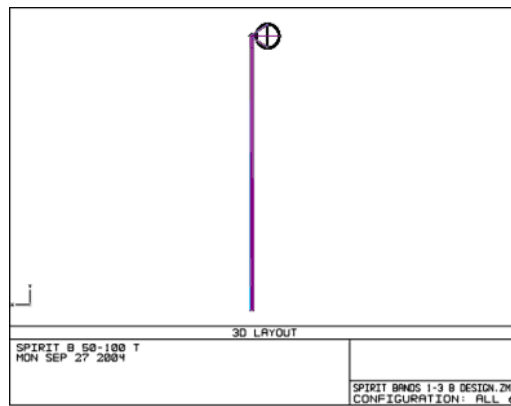


Fig. 1. Ray trace drawing of collector telescope, shown perpendicular to the primary aperture; the boom is along the direction of the rays after leaving the collector.

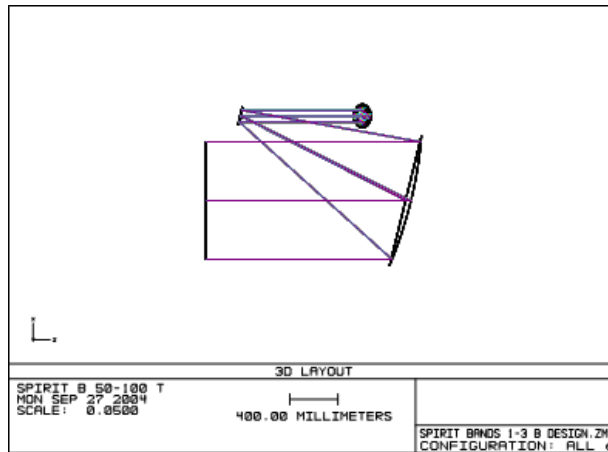


Figure 2 - Ray trace drawing of collector shown perpendicular to the primary mirror

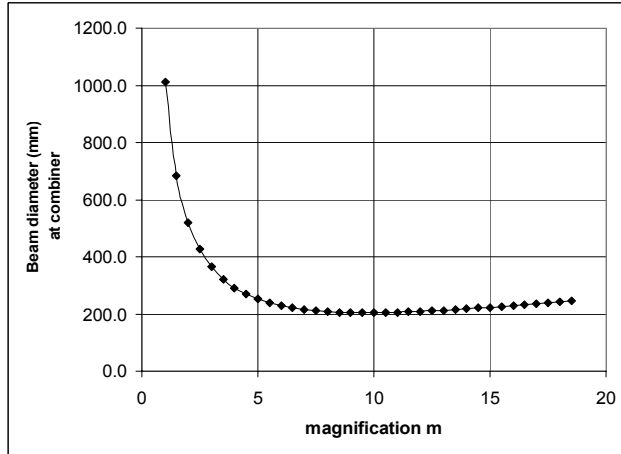


Figure 3 - Graph showing beam size at combiner as a function of m, the collector telescope demagnification

### 2.2 Beam combiner – second stage of beam compression

As Figure 3 indicates, the beam diameter entering the beam combiner volume is approximately 200 mm, beyond the limit of fabrication of the metal mesh beamsplitters. Therefore it was necessary to introduce a second beam compressing telescope. This telescope is also a pair of off axis parabolas, with a demagnification of 4. This was sufficient to allow the metal mesh beamsplitters in the next to last spectral channel to be of feasible size (< 150 mm diameter).

After this beam compression, a dichroic is used to split off near infrared light to the fringe (Zero Path Difference) sensor and angle sensor (see the discussion in Section 2.x). The function of the fringe sensor is to maintain high contrast fringes. The function of the angle sensor is to control pointing of the beams, so that the beams are always overlapping on the final beamsplitter in the Michelson configuration. This sensor uses a fold flat, used for packaging the interferometer optics, to control the direction of the beam. Figure 3 shows the second stage beam compressor and flat mirror.

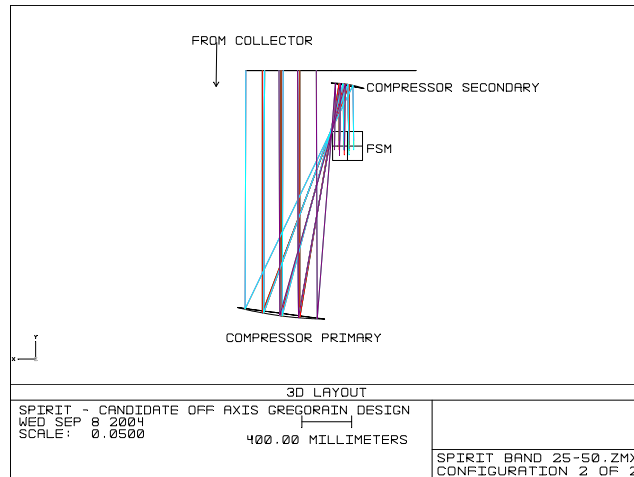


Figure 4 - second stage beam compressor, fine steering mirror

### 2.3 Delay line and interferometer optics

There are 4 science channels in the baseline design, separated by wavelength. The bands are shown in Table 2. In the design the shortest wavelength bands are transmitted first through metal mesh beamsplitters. Figure 5 shows the layout of the different bands. The beam is continuously expanding as it traverses from the first channel to the last, by amount

corresponding to the total beam compression factor (40), keeping the  $A\Omega$  constant for the system; this is equivalent to a field of 40 arcminutes.

In the interferometer design, light from one of the collectors passes through a fixed set of mirrors and metal mesh beamsplitters, the beam from the other passes through a set of movable mirrors as shown in Figure 5<sup>2</sup>. This allows equal optical paths over a large spectral range. The set of 4 roof mirrors shown in the upper portion of Figure 5, are moved with respect to the beamsplitter optics.

The Michelson beamsplitters, located after the metal mesh beamsplitters, have a fused silica substrate. To image the light onto the detectors, there are 2 off axis ellipses, 1 for both the reflected and transmitted outputs, for each channel. In the case of the longest wavelength channels, the final  $f$ /number at the detector is very fast ( $f/3.5$ ) because of a design requirement to Nyquist sample at the center wavelength in each band – see Table I for specific information about each channel.

Specific coatings for the Michelson beamsplitters have not been examined to date.

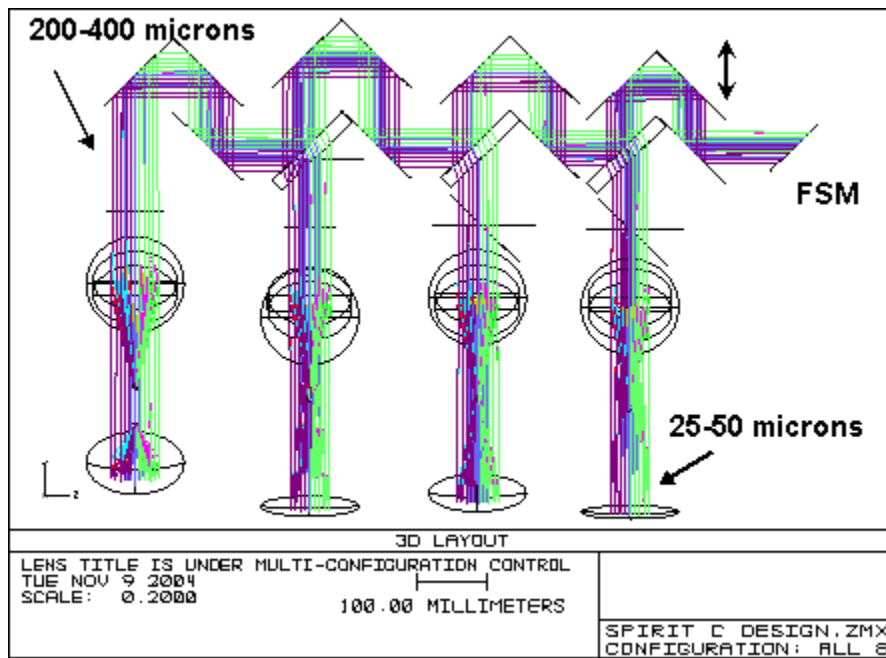


Figure 5 - Top view of 4 channel outputs; both outputs in each channel are captured

Band	Min $\lambda$ ( $\mu\text{m}$ )	Max $\lambda$ ( $\mu\text{m}$ )
1	25	50
2	50	100
3	100	200
4	200	400

Table 2 - Spectral bands

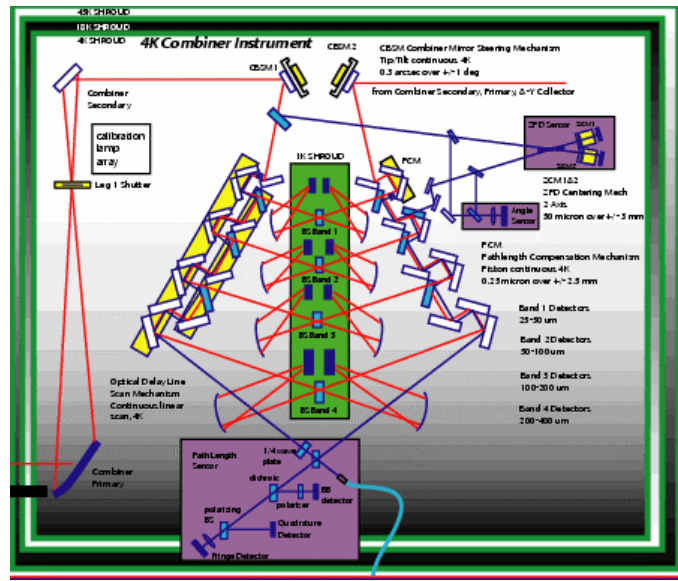


Figure 6 - Functional diagram of optical delay lines plus interferometer optics

2.4 Stray light

For both thermal and optical reasons, it is important to minimize stray light. For the wavelengths at which this instrument operates (25-400 microns), scattering due to mirror roughness and particulate contamination is negligible. The primary concern is thermal infrared radiation emitted by the sunshields and truss. Figure 7 shows the geometry of the system, including sunshield and truss locations. Analysis, using a commercially available software package, was performed to determine where baffles are placed in order to accomplish this. There are four baffles that are useful, one on each of the collector telescopes and one on each side of the combiner. Figures 8&9 show how the lengths of each baffles

Figure 1. C design furthest spacing, baffles not shown

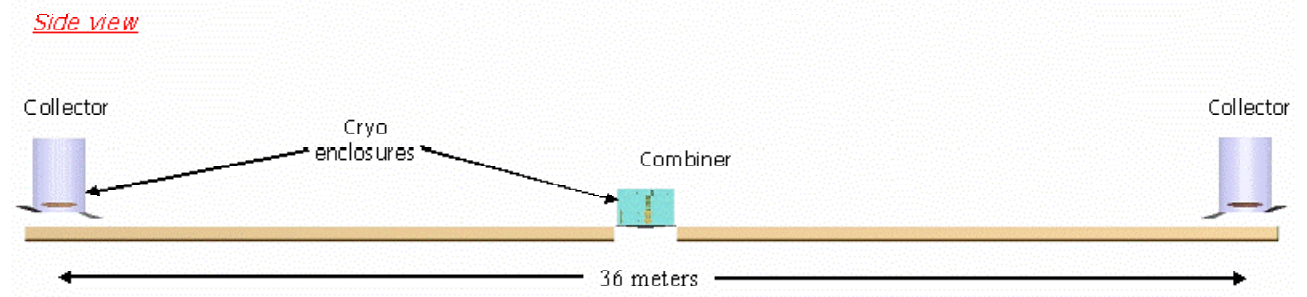


Figure 7 - Stray light geometry

For the collector telescopes, this radiation has the effect of heating the collector telescope assembly. Normally, this would cause the optics to be warmed above the 4K operating temperature. However, the collector optics are being actively cooled to 4K by cryocoolers. Thus the real effect of the radiation is to increase the parasitic heat load on the cryocoolers.

For the combiner module, the chief problem with thermal IR light entering the apertures is that the light may reach the detectors and “wash out” the signal, thus degrading the science.

The best way to mitigate this is to place baffles at the collector telescope exit apertures and the combiner module entrance apertures. Ideally, the baffle lengths would be whatever it takes to completely block the view of the sunshields and truss. For the combiner, shorter baffles were used with reliance on field stops at the foci of the combiner telescopes to reduce stray light to acceptable levels. It is important for science reasons to minimize the baffles, as they combine to limit the minimum baseline that is achievable. See Figures 6 & 7 for calculations of baffle lengths for the combiner and collector, respectively.

In order to calculate numerically the extent of the thermal effects, backwards ray tracing was done – see Figure 8. Assigning a given flux to each ray resulted in the total effects for a given baffle length. The length was varied until an acceptable level was reached.

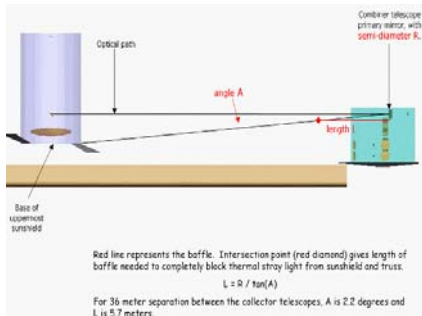


**Figure 8 - Calculating the combiner telescope baffle length**

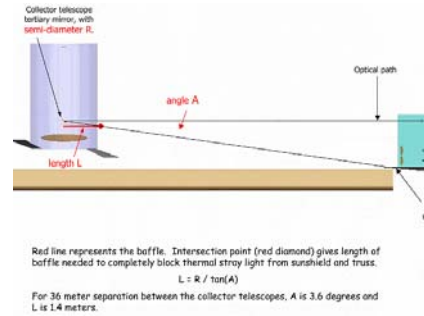


**Figure 9 - Calculating the collector telescope baffle length**

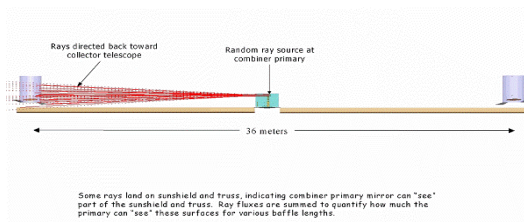


**Figure 10 - Backwards ray trace (combiner- collector)**

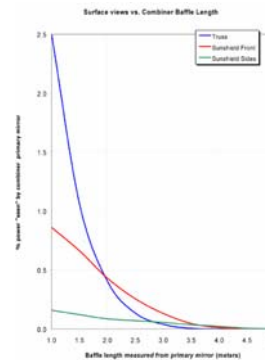


**Figure 11 - Stray light effects at maximum boom length**

## 2.5 Metrology

The metrology subsystem provides the necessary spatial measurements to meet the requirements for control and knowledge of pointing, baseline length and optical path difference, to maintain alignment between the optical beams from the two arms of the science interferometer, and to provide an absolute phase reference. To accomplish this, it directly measures certain dimensions of the opto-mechanical hardware, including separation and relative orientation of the collectors and combiner, and optical path difference between the two interferometer arms. It also makes measurements based on guide stars, including absolute pointing of the spacecraft, white-light fringe sensing, and fine angle sensing. Metrology-specific hardware includes a path-length sensor, angle sensor, zero-path-difference sensor, laser ranging, and tip/tilt sensors.

The metrology requirements are listed in Table 3:

Requirement	Value
Baseline length precision	10 mm
Baseline direction precision	30 arcsec
Collector Coarse Pointing precision	0.5 arcmin
Collector Coarse Pointing range	$\pm 30$ arcmin
Bearing precision	10 arcsec in each axis
Bearing measurement range	$\pm 30$ arcmin in each axis
Distance precision	1 mm
Distance measurement range	3 m to 18 m
Bearing/distance update rate	2 Hz
Fine pointing angle precision	0.1 arcsec on sky
Fine pointing angle measurement range	$\pm 0.5$ arcmin on sky in each axis
Fine pointing angle update rate	2 Hz
Optical path difference precision	0.5 $\mu\text{m}$
Optical path difference accuracy	1 part in $10^7$
Optical path difference measurement range	$\pm 2$ m
Optical path difference update rate	every fringe zero crossing
Zero path difference precision	0.5 $\mu\text{m}$
Zero path difference update rate	2 Hz

**Table 3- Metrology system requirements**

A drawing of the physical measurements being made is shown below

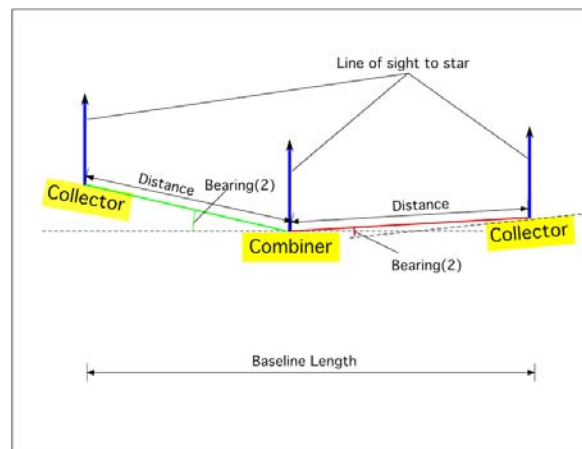


**Figure 12 Physical measurements made by metrology systems**

The requirements for the different metrology sensors are listed below:

Baseline length and orientation

Requirements:

Precision (length)      10 mm  
 Precision (direction)    30 arcsec

Collector Coarse Pointing

Requirements:

Precision: 0.5 arcmin  
 Range: ± 30 arcmin

Bearing/distance (distance and angle from point on one unit to point on another)

Requirements:

Precision (bearing) 10 arcsec in each axis  
 Range (bearing) ± 30 arcmin in each axis  
 Precision (distance) 1 mm  
 Range (distance) 3 m to 18 m  
 Update rate 2 Hz

Fine Pointing Angle (direction of LOS wrt stars, for each arm)

Requirements:

Precision (on the sky) 0.1 arcsec  
 Range (on the sky) ± 0.5 arcmin in each axis  
 Update rate 2 Hz

Optical path difference

Requirements:

Precision 0.5 μm  
 Accuracy 1 part in 107  
 Range ± 2 m  
 Update rate every fringe zero crossing

Zero Path Difference

Requirements:

Precision 0.5 μm  
 Update rate 2 Hz

A functional drawing of the metrology systems is shown below:

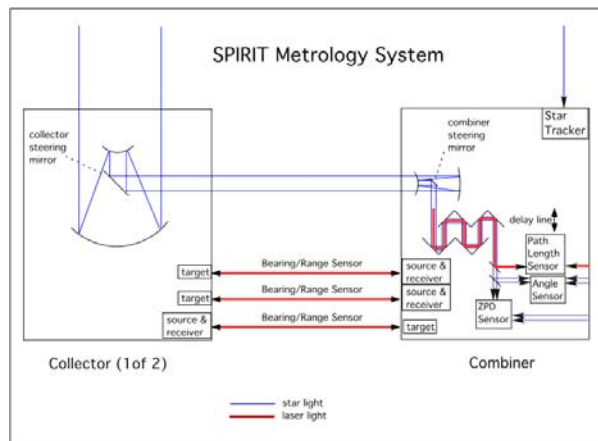


Figure 13 - Functional layout of metrology systems

## 2.6 Optical Testing

There are a number of issues to be addressed in Integration and Test. A primary one is what configuration would allow fringes to be detected at minimum cost. One concept is shown in Figure 14. This concept uses a single, movable source whose light is then collimated and split into two beams via two large flats. The beams are then sent into the beam combiner from a relatively short distance, presumably on the order of 3 meters. Use of these so-called “stub booms” would allow fringes to be produced in the output of the beam combiner, showing optical alignment requirements are being met. Each of the optical subsystems (collecting telescopes, beam combiner, etc.) is tested separately, as would the flight booms and trolleys.

Because of the difficulty of doing hardware validation of the flight system on the ground, integrated modeling is being planned. This is similar to what is being done for the James Webb Space Telescope. Analysis of the sub-system performance parameters are compared to their actual performance under operational conditions in thermal vacuum testing. The system’s predicted analytical performance is verified by demonstrating that the cryogenic performance at the sub-system level, i.e., individual telescopes and mechanisms, and the measured performance of the instrument, i.e. the beam combiner fall within the specified performance parameters at the subsystem and instrument level.

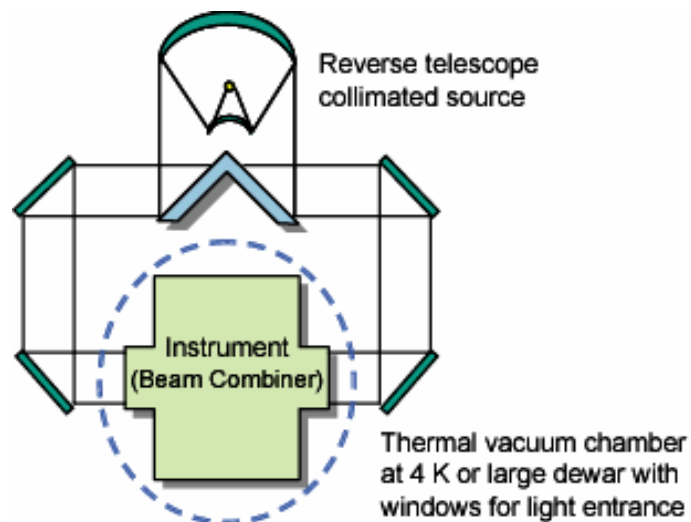


Figure 14 - Optical Testing concept

## 2.7 Summary

The overall optical system design for SPIRIT is presented. The form selected is a pair of Cassegrain, afocal collector telescopes, with a 1 meter aperture and with a 1 arcmin field of view and a maximum 36 meter separation, each followed by a second afocal telescope to further demagnify the beam, followed by a dual port Michelson interferometer. There are 4 spectral wavelength channels, starting at 25 microns and ending at 400 microns. Metal mesh filters are used to separate the wavelength channels. The beam magnification of the collector telescopes is an important design consideration, and a formula is presented which allows an optimum value to be determined. A preliminary stray light study is presented, resulting in minimum baffle sizes to be determined. A concept for optical testing is presented, in which each of the subsystems are measured and integrated modeling techniques are used to validate system performance.

## REFERENCES

1. <sup>[1]</sup> Leisawitz, D., Baker, C., Barger, A., Benford, D., Blain, A., Boyle, R., Broderick, R., Budinoff, J., Carpenter, J., Caverly, R., Chen, P., Cooley, S., Cottingham, C., Crooke, J., DiPietro, D., DiPirro, M., Femiano, M., Ferrer, A., Fischer, J., Gardner, J.P., Hallock, L., Harris, K., Hartman, K., Harwit, M., Hillenbrand, L., Hyde, T., Jones, A., Kellogg, J., Kogut, A., Kuchner, M., Lawson, W., Lecha, J., Lecha, M., Mainzer, A., Mannion, J., Martino, A., Mason, P., Mather, J.C., McDonald, G., Mills, R., Mundy, L., Ollendorf, S., Pellicciotti, J., Quinn, D., Rhee, K., Rinehart, S.A., Sauerwine, T., Silverberg, R.F., Smith, T., Stacey, G., Stahl, H.P., Staguhn, J., Tompkins, S., Tveekrem, J., Wall, S., and Wilson, M., The Space Infrared Interferometric Telescope (SPIRIT): High-resolution imaging and spectroscopy in the far-infrared, *J. Adv. Sp. Res.*, in press (2007), doi:10.1016/j.asr.2007.05.081
2. <sup>[2]</sup> Hyde, T.T., Leisawitz, D.T., and Rinehart, S.A., System engineering the Space Infrared Interferometric Telescope (SPIRIT), *Proc. SPIE 6687*, this volume (2007).
3. <sup>[3]</sup> Budinoff, J.G., Leisawitz, D.T., Rinehart, S.A., DiPirro, M.J., Jones, D.L., Hyde, T.T., and Taylor, B., Mechanical design of the Space Infrared Interferometric Telescope (SPIRIT), *Proc. SPIE 6687*, this volume (2007).
4. <sup>[4]</sup> DiPirro, M.J., Cottingham, C., Boyle, R., Ollendorf, S., and Leisawitz, D.T., The SPIRIT thermal system, *Proc. SPIE 6687*, this volume (2007).
5. <sup>[5]</sup> Benford, D.J., Rinehart, S.A., Hyde, T.T., and Leisawitz, D.T., Cryogenic far-infrared detectors for the Space Infrared Interferometric Telescope (SPIRIT), *Proc. SPIE 6687*, this volume (2007).
6. <sup>[6]</sup> Rinehart, S.A., Armstrong, J.T., Frey, B.J., Jung, J., Kirk, J., Leisawitz, D.T., Leviton, D.B., Lyon, R.G., Martino, A.J., Mundy, L.G., Pauls, T.A., and Schurr, S., Wide-field imaging interferometry: An enabling technique for high angular resolution astronomy, *Proc. SPIE 6687*, this volume (2007).
7. <sup>[7]</sup> Martino, A.J., Leisawitz, D.T., Thompson, A.K., Rinehart, S.A., and Frey, B.J., An optical model of the Wide-field Imaging Interferometry Testbed, *Proc. SPIE 6687*, this volume (2007)
8. <sup>[8]</sup> Crooke, J., Gunderson, J., Hagopian, J., Levine, M., Developing a NASA Strategy for the Verification of Large Space Telescope Observatories, *Proc. SPIE 6271* (2006)
9. <sup>[9]</sup> Mosier, G., Howard, J., Johnston, J., Parrish, K., Hyde, T., McGinnis, M., Bluth, A., Kim, K., Ha, Q., The role of integrated modeling in the design and verification of the James Webb Space Telescope, *Proc. SPIE 5528* (2004)